The Astrophysical Journal Letters, 745:L34 (5pp), 2012 February 1 doi:10.1088/2041-8205/745/2/L34

CLEARING OUT A GALAXY

Kastytis Zubovas and Andrew King
Theoretical Astrophysics Group, University of Leicester, Leicester LE1 7RH, UK; ark@astro.le.ac.uk
Received 2011 November 10; accepted 2011 December 23; published 2012 January 17

ABSTRACT

It is widely suspected that active galactic nucleus (AGN) activity ultimately sweeps galaxies clear of their gas. We work out the observable properties required to achieve this. Large-scale AGN-driven outflows should have kinetic luminosities $\sim\eta\, L_{\rm Edd}/2 \sim 0.05\, L_{\rm Edd}$ and momentum rates $\sim 20\, L_{\rm Edd}/c$, where $L_{\rm Edd}$ is the Eddington luminosity of the central black hole and $\eta \sim 0.1$ its radiative accretion efficiency. This creates an expanding two-phase medium in which molecular species coexist with hot gas, which can persist after the central AGN has switched off. This picture predicts outflow velocities $\sim$1000–1500 km s^{-1} and mass outflow rates up to 4000 $M_\odot$ yr^{-1} on kpc scales, fixed mainly by the host galaxy velocity dispersion (or equivalently black hole mass). All these features agree with those of outflows observed in galaxies such as Mrk231. This strongly suggests that AGN activity is what sweeps galaxies clear of their gas on a dynamical timescale and makes them red and dead. We suggest future observational tests of this picture.

Key words: accretion, accretion disks – black hole physics – galaxies: evolution – quasars: general

1. INTRODUCTION

Recently, three groups (Feruglio et al. 2010; Rupke & Veilleux 2011; Sturm et al. 2011) have used molecular spectral line observations to reveal fast ($v_{\rm out} \sim 1000$ km s^{-1}) kpc-scale, massive ($\dot{M}_{\rm out} \sim 1000\ M_\odot$ yr^{-1}) outflows in the nearby quasar Mrk231. Other galaxies show indications of similar phenomena (e.g., Riffel & Storchi-Bergmann 2011a, 2011b; Sturm et al. 2011). These appear to show how quasar feedback can transform young, star-forming galaxies into red and dead spheroids. All three groups reach this conclusion for Mrk231 essentially by noting that the mass outflow rate $\dot{M}_{\rm out}$ and the kinetic energy rate $\dot{E}_{\rm out} = \dot{M}_{\rm out} v_{\rm out}^2/2$ of the outflow are too large to be driven by star formation, but comparable with those predicted in numerical simulations of active galactic nucleus (AGN) feedback. The kinetic energy rate is a few percent of the likely Eddington luminosity $L_{\rm Edd} = 4\pi GMc/\kappa$ of the central black hole of mass M (where κ is the electron-scattering opacity). The outflowing material must have a multi-phase structure, because $v_{\rm out}$ greatly exceeds the velocity corresponding to the molecular dissociation temperature ($v_{\rm diss} \lesssim 10$ km s^{-1}; see Section 5 below).

In a recent paper (King et al. 2011), we showed that large-scale flows of this type (technically, an energy-driven flow; see Section 3) can indeed drive much of the interstellar gas out of a galaxy bulge on a dynamical timescale $\sim 10^8$ yr, leaving it red and dead, provided that the central supermassive black hole (SMBH) accretes for about twice the Salpeter time after reaching the value set by the M–σ relation. In Power et al. (2011) we showed that the remaining bulge mass is close to the value set by the observed black-hole–bulge-mass relation (e.g., Häring & Rix 2004). However, we did not investigate the observable features of this process, including in particular the way that the interstellar gas is swept up.

We return to this problem here, as it offers a clear observational test of the idea that AGN outflows are responsible for making galaxies red and dead. To keep our treatment as general as possible (specifically, independent of the details of numerical simulations) we adopt a simple analytic approach. We find that this process predicts outflow velocities $\sim$1000–1500 km s^{-1}, and mass outflow rates up to $\sim$4000 $M_\odot$ yr^{-1}, several hundred times the Eddington value, in good agreement with observations. In addition, we find that the observable momentum outflow rate is $\sim$20 times greater than L/c of the driving AGN, also in agreement with observations. We conclude that AGN outflows are good candidates for the agency sweeping galaxies clear of gas.

2. WINDS

To drive outflows with $\dot{E}_{\rm out}$ approaching $L_{\rm Edd}$ at large radius, the active nucleus of a galaxy must somehow communicate this luminosity from its immediate vicinity. Direct transport by radiation is problematic, not least because galaxies are generally optically thin (however, dust opacity may be large enough to absorb this radiation and provide feedback; see Murray et al. 2005). Jets are sometimes invoked, but are relatively inefficient because they tend to drill holes in the interstellar medium (ISM) rather than driving it bodily away. Accordingly, the most likely connection is via high-velocity wide-angle winds expelled from the vicinity of the nucleus by radiation pressure (e.g., Pounds et al. 2003a, 2003b). Recent observations suggest that such winds are very common in AGNs (Tombesi et al. 2010a, 2010b). In this Letter, we use the term "wind" to refer to the mildly relativistic ($v \sim 0.1c$) ejection of accretion disk gas from the immediate vicinity of the SMBH resulting from Eddington accretion, and "outflow" (see Section 4) for the large-scale nonrelativistic flows caused by the interaction between the wind and the galaxy's ambient gas.

The winds have simple properties. With mass rate $\dot{M}_{\rm w} \sim \dot{M}_{\rm Edd}$, where $\dot{M}_{\rm Edd} = L_{\rm Edd}/\eta c^2$ is the Eddington accretion rate and η is the accretion efficiency, a wide-angle wind has scattering optical depth $\sim$1 (King & Pounds 2003), assuming that the covering factor of absorbing gas is close to unity (see the discussion below Equation (2)). So, each driving photon on average scatters about once before escaping to infinity and gives up all of its momentum to the wind, so that the wind mass flow rate $\dot{M}_{\rm w}$ and velocity v obey

$$\dot{M}_{\rm w} v \sim \frac{L}{c}. \quad (1)$$

Defining $\dot{m} = \dot{M}_{\rm w}/\dot{M}_{\rm Edd} \sim 1$ as the Eddington factor of the wind, we immediately find

$$\frac{v}{c} \sim \frac{\eta}{\dot{m}} \sim 0.1 \quad (2)$$

(cf. King 2010). The likely ionization equilibrium of the wind is such that it produces X-rays (King 2010). In line with these expectations, blueshifted X-ray iron absorption lines corresponding to velocities $\sim 0.1c$ are seen in a significant fraction of local AGNs (e.g., Pounds et al. 2003a, 2003b; Tombesi et al. 2010a, 2010b), justifying our assumption of a covering factor close to unity. In all cases the inferred wind mass flow rates agree with Equation (1). So, these black hole winds have momentum and energy rates

$$\dot{P}_w \sim \dot{m}\frac{L_{\rm Edd}}{c} \sim \frac{L_{\rm Edd}}{c}, \quad (3)$$

and

$$\dot{E}_w = \frac{1}{2}\dot{M}_{\rm w}v^2 \sim \frac{\eta}{2\dot{m}}L_{\rm Edd} \sim 0.05\,L_{\rm Edd}, \quad (4)$$

where we have used Equations (1) and (2) in Equation (4).

3. SHOCKS

The expression (4) for the energy rate of a black hole wind is obviously promising for driving the observed large-scale outflows. Although the ISM is clumpy, the outflow bubble inflated by the wind easily sweeps past the clumps, affecting the diffuse gas (e.g., Mac Low & McCray 1988). Furthermore, the clouds are shocked by the passing outflow and evaporate inside the hot wind bubble (Cowie & McKee 1977), so most of their material also joins the outflow. A detailed treatment of the interaction between the clumpy ISM and the wind-driven outflow is beyond the scope of this paper, although we address some of the implications in Section 6. In the present analysis, we assume that most of the sightlines from the SMBH are covered with diffuse medium, irrespective of whether they are also obscured by clumps.

The question now is how efficiently the wind energy is transmitted to the outflow. This depends crucially on how the wind interacts with the diffuse ISM of the host galaxy. Since the wind is hypersonic, it must decelerate violently in a reverse shock and simultaneously drive a forward shock into the host ISM. There are two possible outcomes, which are realized under different conditions in galaxies.

The first outcome (momentum-driven flow) occurs if the shocked wind gas can cool on a timescale short compared with the motion of the shock pattern. In this case the shocked wind gas is compressed to high density and radiates away almost all of the wind kinetic energy (i.e., $\dot{E}_{\rm out} \ll \dot{E}_w = (\eta/2\dot{m})\,L_{\rm Edd}$). This shocked wind has gas pressure equal to the pre-shock ram pressure $\dot{P}_{\rm w} \simeq L_{\rm Edd}\dot{m}/c \propto M$, and this pushes into the host ISM.

The second case (energy-driven flow) occurs if the shocked wind gas is not efficiently cooled and instead expands as a hot bubble. Then the flow is essentially adiabatic and has the wind energy rate, i.e., $\dot{E}_{\rm out} \simeq \dot{E}_{\rm w} = (\eta/2\dot{m})\,L_{\rm Edd} \sim 0.05\,L_{\rm Edd}$ (from Equation (4)). The hot bubble's thermal expansion makes the driving into the host ISM more vigorous than in the momentum-driven case. Observed galaxy-wide molecular outflows must be energy-driven, as demonstrated directly by their kinetic energy content (cf. Equation (4)).

Which of these two very different cases occurs at a given point depends on the cooling of the shocked gas. It is easy to show that the usual atomic cooling processes (free–free and free–bound radiation) are negligible in all cases. The dominant process tending to cool the shocked black hole wind is the inverse Compton effect (Ciotti & Ostriker 1997). The quasar radiation field is much cooler than the wind shock temperature (typically $\sim 10^7$ K and $\sim 10^{11}$ K, respectively), and so cools the shocked wind provided that it is not too diluted by distance. Equations (8) and (9) of King (2003) show that this holds if and only if the shock is at distances $R \lesssim 1$ kpc from the active nucleus, since the Compton cooling time goes as R^2 and the flow time typically as R. So we expect momentum-driven flow close to the nucleus, and energy-driven flow if gas can be driven far away from it.

We note that Silk & Nusser (2010) claim that an energy-driven flow never occurs. However, they seem to have considered the cooling of the ambient gas, rather than the shocked wind and swept-up ISM: the cooling function they use extends only to temperatures $\sim 10^7$ K, rather than the wind shock temperature $\sim 10^{11}$ K—see King et al. (2011) for details.

4. OUTFLOWS

For an isothermal ISM density distribution with velocity dispersion σ and gas fraction f_c (the ratio of gas density to background potential density) one can solve analytically the equation of motion for the shock pattern for both momentum-driven flow (King 2003, 2005) and energy-driven flow (King 2005; King et al. 2011).

In the momentum-driven case there are two distinct flow patterns, depending on the black hole mass M. For $M < M_\sigma$, where

$$M_\sigma = \frac{f_c\kappa}{\pi G^2}\sigma^4 \simeq 4\times 10^8\,M_\odot\sigma_{200}^4 \quad (5)$$

(with $f_c = 0.16$ (its cosmological value) and $\sigma_{200} = \sigma/(200\,{\rm km\,s^{-1}})$) the wind momentum is too weak to drive away the swept-up ISM and the flow stalls at some point. For $M > M_\sigma$, the wind momentum drives the swept-up matter far from the nucleus. It is intuitively reasonable to assume that the black hole cannot easily grow its mass significantly beyond the point where it expels the local interstellar gas in this way, i.e., beyond M_σ. Equation (5) is very close to the observed M–σ relation, despite having no free parameter. Detailed calculations (Power et al. 2011) show that the SMBH is likely to grow for 1–2 additional Salpeter times after it reaches M_σ, increasing its final mass by a factor of a few. This process is even more pronounced at higher redshift, as then it takes longer for the outflow to clear the galaxy, so the SMBH must be active for longer.

We conclude that outflows drive gas far from the nucleus, and thus become energy-driven, once $M \gtrsim M_\sigma$. This is evidently the case needed to explain the molecular outflows seen in Mrk231 and other galaxies.

5. LARGE-SCALE FLOWS

In an energy-driven flow the adiabatic expansion of the shocked wind pushes the swept-up ISM in a "snowplow." King et al. (2011) derive the analytic solution for the expansion of the shocked wind in a galaxy bulge with an isothermal mass distribution. With AGN luminosity $l\,L_{\rm Edd}$, all such solutions tend to an attractor

$$\dot{R} = v_e \simeq \left[\frac{2\eta l f_c}{3 f_g}\sigma^2 c\right]^{1/3} \simeq 925\sigma_{200}^{2/3}(l f_c/f_g)^{1/3}\,{\rm km\,s^{-1}} \quad (6)$$

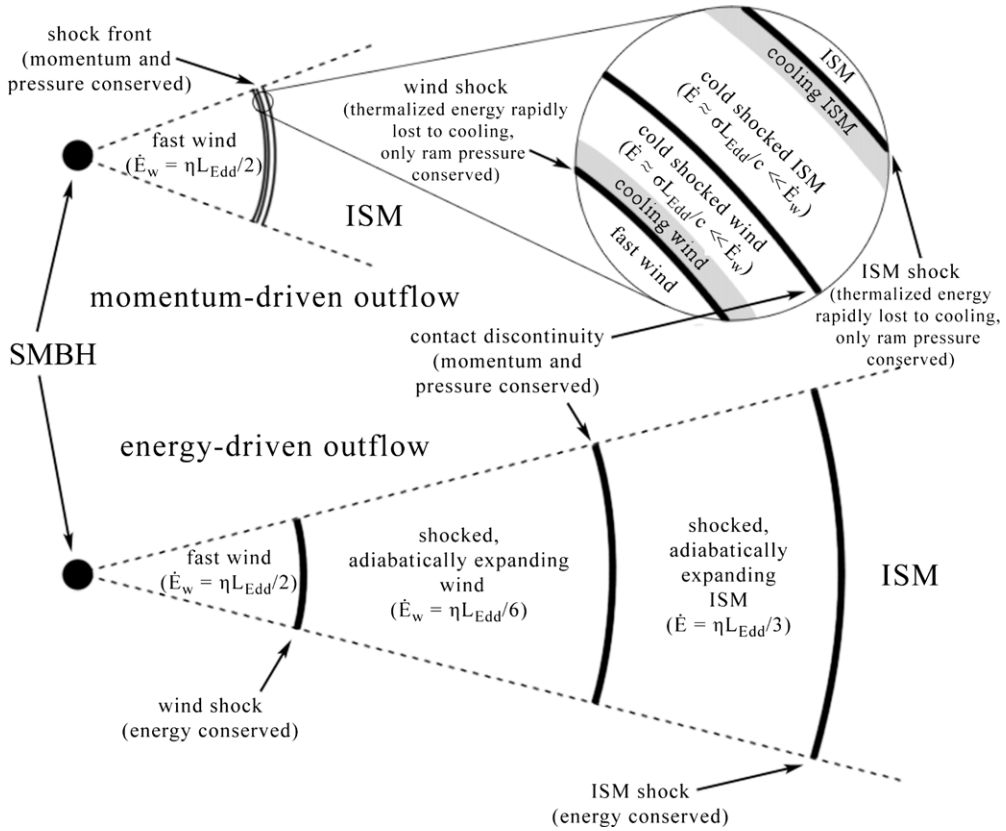

Figure 1. Diagram of momentum-driven (top) and energy-driven (bottom) outflows. In both cases a fast wind (velocity $\sim \eta c \sim 0.1c$) impacts the interstellar gas of the host galaxy, producing an inner reverse shock slowing the wind, and an outer forward shock accelerating the swept-up gas. In the momentum-driven case, the shocks are very narrow and rapidly cool to become effectively isothermal. Only the ram pressure is communicated to the outflow, leading to very low kinetic energy $\sim(\sigma/c)\, L_{\rm Edd}$. In an energy-driven outflow, the shocked regions are much wider and do not cool. They expand adiabatically, communicating most of the kinetic energy of the wind to the outflow (in simple cases approximately 1/3 is retained by the shocked wind). The outflow radial momentum flux is therefore greater than that of the wind. Momentum-driven flows occur when shocks happen within $\sim$1 kpc of the AGN, and establish the M–σ relation (King 2003, 2005). Once the supermassive black hole mass attains the critical M–σ value, the shocks move further from the AGN and the outflow becomes energy-driven. This produces the observed large-scale flows, which probably sweep the galaxy clear of gas.

until the central AGN luminosity decreases significantly at some radius $R = R_0$, when the expansion speed decays as

$$\dot{R}^2 = 3\left(v_e^2 + \frac{10}{3}\sigma^2\right)\left(\frac{1}{x^2} - \frac{2}{3x^3}\right) - \frac{10}{3}\sigma^2, \qquad (7)$$

where $x = R/R_0 \geqslant 1$. In Equation (6), f_g is the gas fraction relative to all matter. This may be lower than the value f_c prevailing when the earlier momentum-driven outflow establishes the M–σ relation (5), as gas may be depleted through star formation, for example.

The solutions (6) and (7) describe the motion of the contact discontinuity where the shocked wind encounters swept-up interstellar gas (see Figure 1). The observed molecular lines are likely to come from the shocked interstellar gas ahead of this discontinuity—its temperature is much lower ($\sim 10^7$ K) than that of the shocked wind, as we shall see. The outer shock must run ahead of the contact discontinuity into the ambient ISM in such a way that the velocity jump across it is a factor of $(\gamma + 1)/(\gamma - 1)$ (where γ is the specific heat ratio). This fixes its velocity as

$$v_{\rm out} = \frac{\gamma + 1}{2}\dot{R} \simeq 1230\sigma_{200}^{2/3}\left(\frac{l f_c}{f_g}\right)^{1/3} \ {\rm km\ s^{-1}} \qquad (8)$$

(where we have used $\gamma = 5/3$ in the last form). This corresponds to a shock temperature of order 10^7 K for the forward shock into the ISM (as opposed to $\sim 10^{10}$–10^{11} K for the wind shock). Since the outer shock and the contact discontinuity are very close together when energy-driven flow starts (see Figure 1) this means that the outer shock is always at

$$R_{\rm out} = \frac{\gamma + 1}{2}R. \qquad (9)$$

The outflow rate of shocked interstellar gas is

$$\dot{M}_{\rm out} = \frac{dM(R_{\rm out})}{dt} = \frac{(\gamma + 1) f_{\rm g}\sigma^2}{G}\dot{R}. \qquad (10)$$

Assuming $M = M_\sigma$, the wind outflow rate is

$$\dot{M}_{\rm w} \equiv \dot{m}\dot{M}_{\rm Edd} = \frac{4 f_c \dot{m}\sigma^4}{\eta c G}. \qquad (11)$$

We can now define a mass-loading factor for the outflow, which is the ratio of the mass flow rate in the shocked ISM to that in the wind:

$$f_{\rm L} \equiv \frac{\dot{M}_{\rm out}}{\dot{M}_{\rm w}} = \frac{\eta(\gamma + 1)}{4\dot{m}}\frac{f_g}{f_c}\frac{\dot{R}c}{\sigma^2}. \qquad (12)$$

Then the mass outflow rate is

$$\dot{M}_{\rm out} = f_{\rm L}\dot{M}_{\rm w} = \frac{\eta(\gamma + 1)}{4}\frac{f_g}{f_c}\frac{\dot{R}c}{\sigma^2}\dot{M}_{\rm Edd}. \qquad (13)$$

Table 1
Observed Outflow Parameters

Object	$M_{\rm BH}$ ($M_\odot$)	σ (km s^{-1})	$L_{\rm bol}$ (erg s^{-1}) (l)	$\dot{M}_{\rm out}$ ($M_\odot$ yr^{-1})	$v_{\rm out}$ (km s^{-1})
Mrk231[a]	4.7×10^{7}[b]	120[b]	45.69[c](0.80)	420	1100
Mrk231[d]	4.7×10^{7}	120	45.69(0.80)	700	750
Mrk231[e]	4.7×10^{7}	120	46.04[f](1.8)	1200	1200
IRAS 08572+3915[e]	$\sim 4.5 \times 10^{7}$*	120***	45.66(1*)	970	1260
IRAS 13120–5453[e]	5.3×10^{6}*	70***	44.83(1*)	130	860
IRAS 17208–0014[e]**	–	–	45.11($\ll 1$)	90	370
Mrk1157[g]	8.3×10^{6}	100	42.57(3.4×10^{-3})	6	350
2QZJ002830.4-281706[h]	5.1×10^{9}[i]	385***	46.58(5.8×10^{-2})	2000	2000

Notes. Outflows observed in molecular gas (Mrk231, IRAS 08572+3915, IRAS 13120–5453, and IRAS 17208–0014), and warm ionized gas (Mrk1157, 2QZJ002830.4-281706). (*) The AGN is assumed to be radiating at its Eddington limit; (**) The galaxy is starburst dominated (Riffel & Storchi-Bergmann 2011b), so we expect a low Eddington factor and hence make no estimates; (***) The SMBH is assumed to lie on the M–σ relation; note that this may be questionable in some cases (cf. McConnell et al. 2011).

References. [a]Rupke & Veilleux 2011; [b]Tacconi et al. 2002; [c]Lonsdale et al. 2003; [d]Feruglio et al. 2010; [e]Sturm et al. 2011; [f]Veilleux et al. 2009; [g]Riffel & Storchi-Bergmann 2011b; [h]Cano-Diaz et al. 2011; [i]Shemmer et al. 2004.

Table 2
Observationally Derived versus Theoretically Predicted Outflow Parameters

Object	$\frac{\dot{E}_{\rm out}}{0.05\,L_{\rm bol}}$	$\frac{\dot{M}_{\rm out} v_{\rm out} c}{L_{\rm bol}}$	$f_{\rm L} \equiv \frac{\dot{M}_{\rm out}}{\dot{M}_{\rm acc}}$	$f_{\rm L,pred.}$	$\dot{M}_{\rm pred.}$ ($M_\odot$ yr^{-1})	$v_{\rm pred.}$ (km s^{-1})
Mrk231	0.66	18	$490 = 22^2$	840	880	810
Mrk231	0.51	20	$820 = 29^2$	840	880	810
Mrk231	1.0	25	$1400 = 37^2$	1110	1150	1060
IRAS 08572+3915	2.1	50	$1200 = 35^2$	910	950	875
IRAS 13120–5453	0.88	31	$1080 = 33^2$	1870	220	610
IRAS 17208–0014	0.06	4.9	$396 = 20^2$	–	–	–
Mrk1157	1.3	110	$9270 = 96^2$	170	85	115
2QZJ002830.4−281706	1.3	20	$307 = 17.5^2$	74	8200	740

Notes. The first three columns give quantities derived from observations of large-scale outflows summarized in Table 1. The last three columns give the mass-loading parameter, mass sweep-out rate, and terminal velocity predicted by our Equations (14), (15), and (8), respectively. We assume the simplest case of an isotropic outflow. Collimation would reduce the predicted mass outflow rate and increase the predicted outflow velocity. With one outlier (see below), the outflow kinetic energy is always very close to 5% of $L_{\rm bol}$ (1st column) as predicted by Equation (4), and the momentum loading (2nd column) is always very similar to the square root of the mass loading (right-hand side of 3rd column), as predicted by Equation (18). It is striking that the relation holds for local quasars (Mrk231), high-redshift quasars (2QZJ002830.4-281706), and low luminosity galaxies (Mrk1157). The last two columns can be directly compared with the last two columns of Table 1; the discrepancies arise due to strong outflow collimation. The only significant outlier, IRAS 17208–0014, is known to be a starburst-dominated galaxy, so we would not expect the outflow to be dominated by the AGN contribution.

If the AGN is still radiating at a luminosity close to Eddington, we have $\dot{R} = v_e$, and using (6) gives

$$f_{\rm L} = \left(\frac{2\eta c}{3\sigma}\right)^{4/3} \left(\frac{f_g}{f_c}\right)^{2/3} \frac{l^{1/3}}{\dot{m}} \simeq 460\sigma_{200}^{-4/3} \frac{l^{1/3}}{\dot{m}}, \quad (14)$$

and

$$\dot{M}_{\rm out} \simeq 3700\sigma_{200}^{8/3} l^{1/3}\ M_\odot\ {\rm yr}^{-1} \quad (15)$$

for typical parameters, $f_{\rm g} = f_{\rm c}$ and $\gamma = 5/3$. If the central quasar is no longer active, the mass outflow rate evidently declines as $\dot{R}/v_e$ times this expression, with $\dot{R}$ given by Equation (7).

It is easy to check from Equations (8) and (15) that the approximate equality

$$\frac{1}{2}\dot{M}_{\rm w} v_{\rm w}^2 \simeq \frac{1}{2}\dot{M}_{\rm out} v_{\rm out}^2 \quad (16)$$

holds, i.e., most of the wind kinetic energy ultimately goes into the mechanical energy of the outflow, as expected for energy driving. One can show from the equations in King (2005) that if the quasar is still active and accreting close to its Eddington rate, the shocked wind retains 1/3 of the total incident wind kinetic energy $\dot{M}_{\rm w} v_{\rm w}^2/2$, giving 2/3 to the swept-up gas. The energy retained in the wind and the swept-up gas has potentially observable emission signatures (see discussion).

Equation (16) means that the swept-up gas must have a momentum rate greater than the Eddington value $L_{\rm Edd}/c$, since we can rewrite it as

$$\frac{\dot{P}_{\rm w}^2}{2\dot{M}_{\rm w}} \simeq \frac{\dot{P}_{\rm out}^2}{2\dot{M}_{\rm out}}, \quad (17)$$

where the $\dot{P}$ are the momentum fluxes. With $\dot{P}_{\rm w} = L_{\rm Edd}/c$, we have

$$\dot{P}_{\rm out} = \dot{P}_{\rm w}\left(\frac{\dot{M}_{\rm out}}{\dot{M}_{\rm w}}\right)^{1/2} = \frac{L_{\rm Edd}}{c} f_{\rm L}^{1/2} \sim 20\sigma_{200}^{-2/3} l^{1/6} \frac{L_{\rm Edd}}{c}, \quad (18)$$

where $f_{\rm L}$ is the mass loading factor of the outflow. The factor $f_{\rm L}^{1/2} \sim 20$ is the reason why observations consistently show $\dot{M}_{\rm out} v_{\rm out} > L_{\rm Edd}/c$.

6. DISCUSSION

We have shown that large-scale outflows driven by wide-angle AGN winds should have typical velocities $v_{\rm out} \sim$ 1000–1500 km s^{-1} and mass flow rates up to $\dot{M}_{\rm out} \sim$ 4000 $M_\odot$ yr^{-1} (Equations (8) and (15)) if the central quasar is still active, with lower values if it has become fainter. Our Equations (8) and (15) directly relate the outflow velocities and mass rates to the properties of the host galaxy. The outflows should have mechanical luminosities $\dot{E}_{\rm out} \sim (\eta/2)\, L_{\rm Edd} \sim 0.05\, L_{\rm Edd}$, but (scalar) momentum rates $\dot{P}_{\rm out} \sim 20\, L_{\rm Edd}/c$. These predictions agree well with observations (see Tables 1 and 2). We conclude that AGN outflows may well be what sweeps galaxies clear of gas.

Our picture predicts several other features that may aid in interpreting observations. It suggests that the molecular outflows come from clumps of cool gas embedded in the outflowing shocked ISM. They are entrained by the advancing outer shock front and persist for a long time. We note that this shock front is Rayleigh–Taylor stable since interstellar gas is compressed here. Further, the temperature of the shocked ISM is in the right range for thermal instability (McKee & Ostriker 1977), and Richtmyer–Meshkov instabilities (Kane et al. 1999) induced by the forward shock mean that new cold clumps may form in the outflow behind it. Simulations by K. Zubovas & S. Nayakshin (2012, in preparation) show that up to 10% of the total mass in the outflow may be locked up in this cold phase. This agrees with the conversion factor of ∼10% used in the papers cited in Table 1 to estimate the total mass outflow rate from observed molecular species. Our model therefore predicts both the total mass outflow rates (Equation (15)) and the observational signatures used to estimate them, in good agreement with observation (Table 2).

The inner wind shock presumably accelerates cosmic-ray particles, and gamma rays result when these hit the colder ISM and shocked wind. The outflows are therefore directly comparable with the gamma-ray emitting bubbles in our Galaxy recently discovered by *Fermi* (Su et al. 2010). One can interpret these as relics of the Milky Way's last quasar outburst about 6 Myr ago by noting that the greater density of the Galactic plane must pinch a quasi-spherical quasar outflow into a bipolar shape (Su et al. 2010; Zubovas et al. 2011). The gamma-ray emission from distant galaxies discussed here should be intrinsically stronger than in the Milky Way, but the long integration time required to detect the Galactic bubbles means that these outflows may be undetectable with current instruments.

Perhaps more promisingly, these cosmic-ray electrons cool and emit synchrotron radiation in the radio band. This radiation may be observable and so it would be interesting to check whether there are kpc or sub-kpc scale radio bubbles associated with the outflows.

We thank Sylvain Veilleux and David Rupke for helpful discussions, and the referee for a very thoughtful and helpful report. Research in theoretical astrophysics at Leicester is supported by an STFC Rolling Grant. K.Z. is supported by an STFC research studentship.

REFERENCES

Cano-Diaz, M., Maiolino, R., Marconi, A., et al. 2011, arXiv:1112.3071
Ciotti, L., & Ostriker, J. P. 1997, ApJ, 487, L105
Cowie, L. L., & McKee, C. F. 1977, ApJ, 211, 135
Feruglio, C., Maiolino, R., Piconcelli, E., et al. 2010, A&A, 518, L155
Häring, N., & Rix, H.-W. 2004, ApJ, 604, L89
Kane, J., Drake, R. P., & Remington, B. A. 1999, ApJ, 511, 335
King, A. 2003, ApJ, 596, L27
King, A. 2005, ApJ, 635, L121
King, A. R. 2010, MNRAS, 402, 1516
King, A. R., & Pounds, K. A. 2003, MNRAS, 345, 657
King, A. R., Zubovas, K., & Power, C. 2011, MNRAS, 415, L6
Lonsdale, C. J., Lonsdale, C. J., Smith, H. E., & Diamond, P. J. 2003, ApJ, 592, 804
Mac Low, M.-M., & McCray, R. 1988, ApJ, 324, 776
McConnell, N. J., Ma, C.-P., Gebhardt, K., et al. 2011, Nature, 480, 215
McKee, C. F., & Ostriker, J. P. 1977, ApJ, 218, 148
Murray, N., Quataert, E., & Thompson, T. A. 2005, ApJ, 618, 569
Pounds, K. A., King, A. R., Page, K. L., & O'Brien, P. T. 2003a, MNRAS, 346, 1025
Pounds, K. A., Reeves, J. N., King, A. R., et al. 2003b, MNRAS, 345, 705
Power, C., Zubovas, K., Nayakshin, S., & King, A. R. 2011, MNRAS, 413, L110
Riffel, R. A., & Storchi-Bergmann, T. 2011a, MNRAS, 411, 469
Riffel, R. A., & Storchi-Bergmann, T. 2011b, MNRAS, 417, 2752
Rupke, D. S. N., & Veilleux, S. 2011, ApJ, 729, L27
Shemmer, O., Netzer, H., Maiolino, R., et al. 2004, ApJ, 614, 547
Silk, J., & Nusser, A. 2010, ApJ, 725, 556
Sturm, E., González-Alfonso, E., Veilleux, S., et al. 2011, ApJ, 733, L16
Su, M., Slatyer, T. R., & Finkbeiner, D. P. 2010, ApJ, 724, 1044
Tacconi, L. J., Genzel, R., Lutz, D., et al. 2002, ApJ, 580, 73
Tombesi, F., Cappi, M., Reeves, J. N., et al. 2010a, A&A, 521, A57
Tombesi, F., Sambruna, R. M., Reeves, J. N., et al. 2010b, ApJ, 719, 700
Veilleux, S., Rupke, D. S. N., Kim, D.-C., et al. 2009, ApJS, 182, 628
Zubovas, K., King, A. R., & Nayakshin, S. 2011, MNRAS, 415, L21